

# Fatigue of Kaowool reinforced aluminum: Effect of shot particle wall thickness

A. AL-OSTAZ

*Civil Engineering Department, University of Mississippi, University, MS 38677, USA*  
E-mail: [alostaz@olemiss.edu](mailto:alostaz@olemiss.edu)

W. J. BAXTER

*GM Research and Development Center, Warren, MI 48090-9055, USA*

I. JASIUK

*The G. W. W. School of Mechanical Engineering, Georgia Institute of Technology, Atlanta, GA 30332-0405, USA*

The fatigue performance of Kaowool fiber reinforced 339 aluminum composites at 300°C is limited by spherical thin walled hollow Kaowool shot particles. These act as crack initiation sites particularly when located at the surface. This problem does not occur for thick walled particles or particles filled with the aluminum matrix. The effect of wall thickness ( $t$ ) is evaluated from finite element analysis of both 2D and 3D models, with and without plasticity. Both models predict that hollow thin walled particles act as defects, while thick walled particles act as reinforcements, this transition being defined by a critical wall thickness ( $t_c$ ). The 3D model is preferred in that it predicts more accurate and smaller values of  $t_c$ . Specifically, the 3D elastic/plastic model predicts that the largest stress concentration occurs for a fractional surface particle and that in this condition  $t_c = 0.18a$ , where  $a$  is the particle radius. This value agrees with our experimental observation that particles with  $t > 0.2a$  do not initiate failures. © 2003 Kluwer Academic Publishers

## 1. Introduction

The addition of discontinuous Kaowool<sup>1</sup> (47Al<sub>2</sub>O<sub>3</sub> 53SiO<sub>2</sub>) fibers substantially increases both the tensile strength [1, 2] and fatigue strength of 339 aluminum at 300°C [3]. However, while the ultimate tensile strength of these composites equals the theoretical value for a perfectly bonded system [1], the fatigue life is limited by the presence of hollow empty thin walled Kaowool shot particles, which are typically spherical and act as sites for crack initiation. These particles range from 20 to 100 μm in diameter, but a detailed study of the fracture surfaces showed that while the failure initiated at a particle located at or near the free surface, the particle size had no discernible effect on the fatigue life. In our initial analysis of this problem [3, 4], these particles were represented by a 2D finite element model of a spherical hollow shell embedded in an elastic aluminum matrix. We calculated the stress distribution in the vicinity of such a hollow particle under the application of an applied stress, and simplified the analysis by focusing attention on the locations corresponding to stress maxima in both the Kaowool shell and the surrounding aluminum matrix. At these locations the stress component parallel to the applied stress was dominant and was used to represent the results. This simple model showed that a critical parameter is the distance ( $d$ ) of

the particle from the free surface. As the distance from the surface decreases, the stress concentration factor (SCF) in the aluminum matrix, adjacent to the particle, increases substantially and attains a maximum value when a small portion of the particle has been removed by machining. This relationship between  $d$  and the SCF was in excellent agreement with the locations of the particles observed at the fatigue crack initiation sites and justified the simplifications in our analysis.

In this paper we also show that the fatigue performance depends on the wall thickness of the shot particles. This effect is described qualitatively by our earlier simple 2D elastic model, but a quantitative correlation with the experimental observations requires a more realistic 3D model, which includes the plasticity of the aluminum matrix.

## 2. Experimental

Composites of 339 aluminum (12Si1Mg1Cu1Ni 0.5Fe wt pct), reinforced by 15 percent Kaowool fibers with an average aspect ratio of 20, were produced by squeeze casting and aged for  $h$  hours at 210°C prior to machining of cylindrical specimens. The gate sections were polished with diamond paste parallel to the axis to avoid perpendicular circumferential scratches. Prior to

<sup>1</sup>Kaowool is a trademark of Thermal Ceramics, Inc., Augusta, Georgia.

fatigue testing at 300°C, the specimens were overaged for 200 hrs at 300°C to stabilize the microstructure. The axial fatigue tests were conducted under load control with fully reversed loading ( $R = -1$ ) at a frequency of 30 Hz. After fatigue failure, both fracture surfaces of each sample were examined by both optical and scanning electron microscopy to identify the fracture origins.

The fatigue experiments were designed to compare two types of composite (hereafter referred to as Types I and II) with different shot particle content and range of

wall thickness. They were characterized by surveying an area of  $\sim 20 \text{ mm}^2$  on a polished section of each casting by both optical and scanning electron microscopy.

### 3. Shot particle concentrations

Typical shot particles are illustrated by the micrographs in Figs 1 to 3. In some cases, scanning electron microscopy was required to obtain a clearer image of the wall thickness (Fig. 3a) or to verify that the particle was solid (Fig. 3b). The particles are approximately

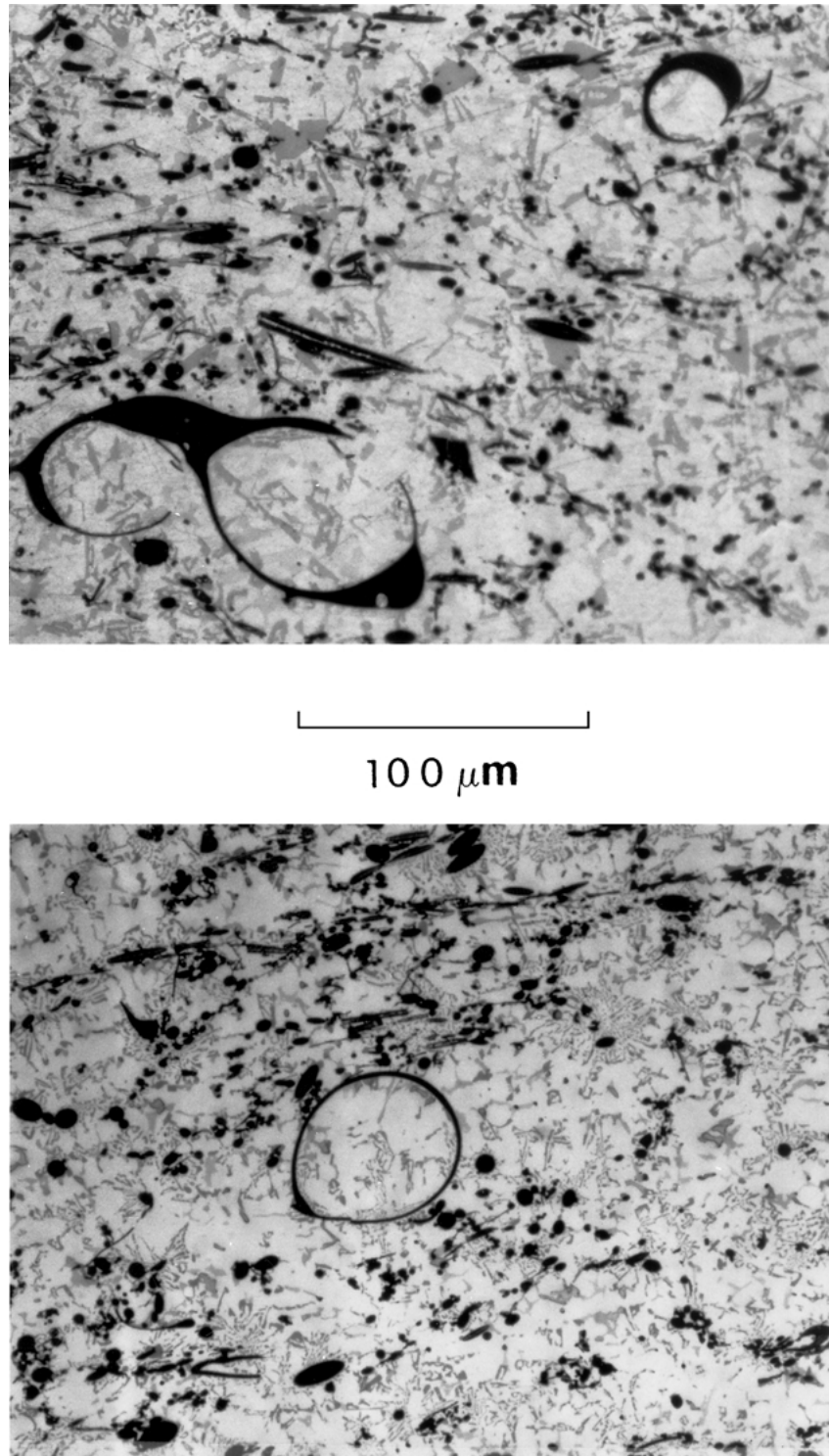


Figure 1 Optical micrographs of a Type I composite showing typical thin-walled shot particles filled with the matrix 339 aluminum. Kaowool fibers and particles appear black. The small particles in the aluminum matrix are primarily Si.

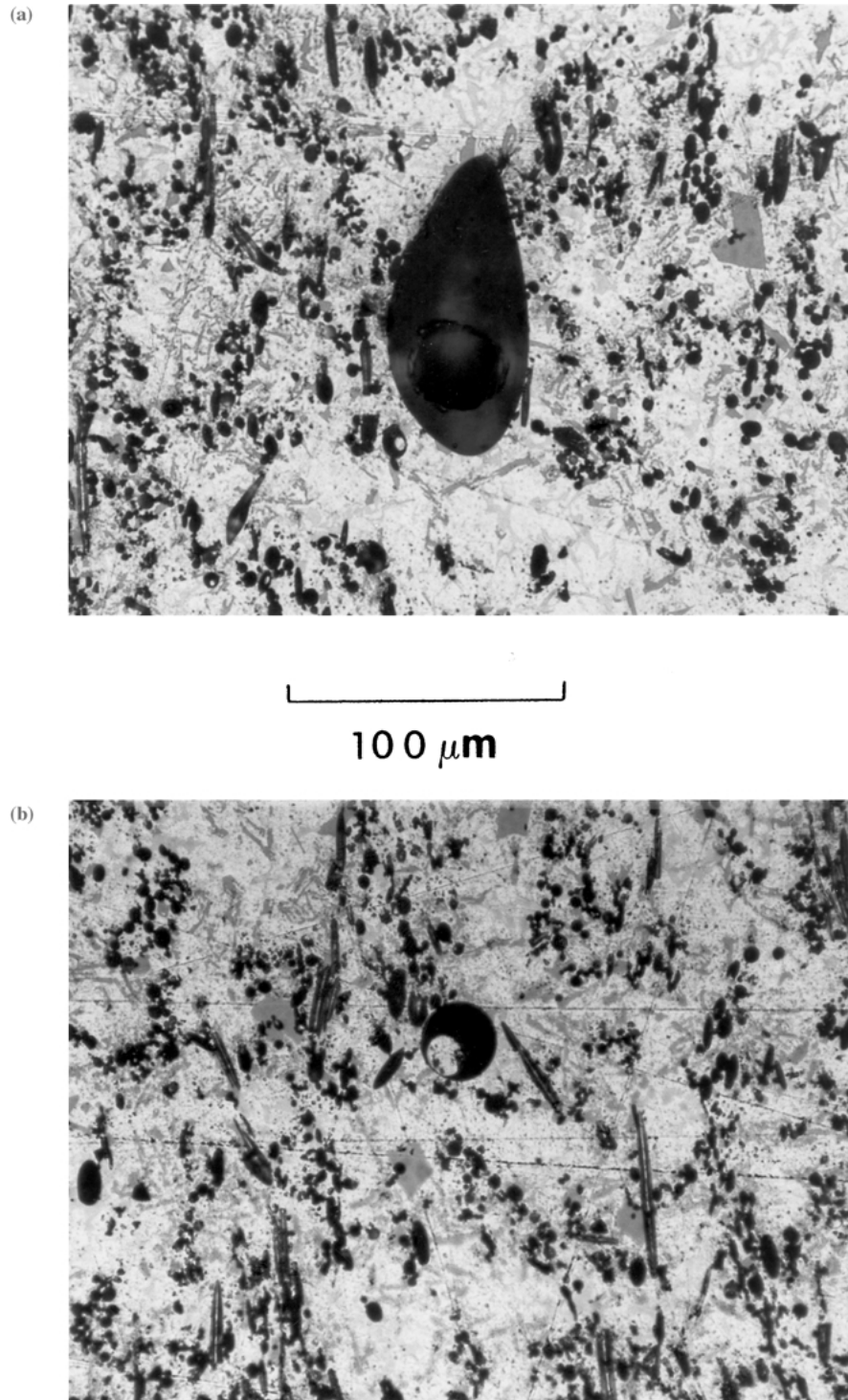


Figure 2 Optical micrographs of a Type II composite showing typical thick-walled shot particles: (a) hollow and (b) filled with aluminum.

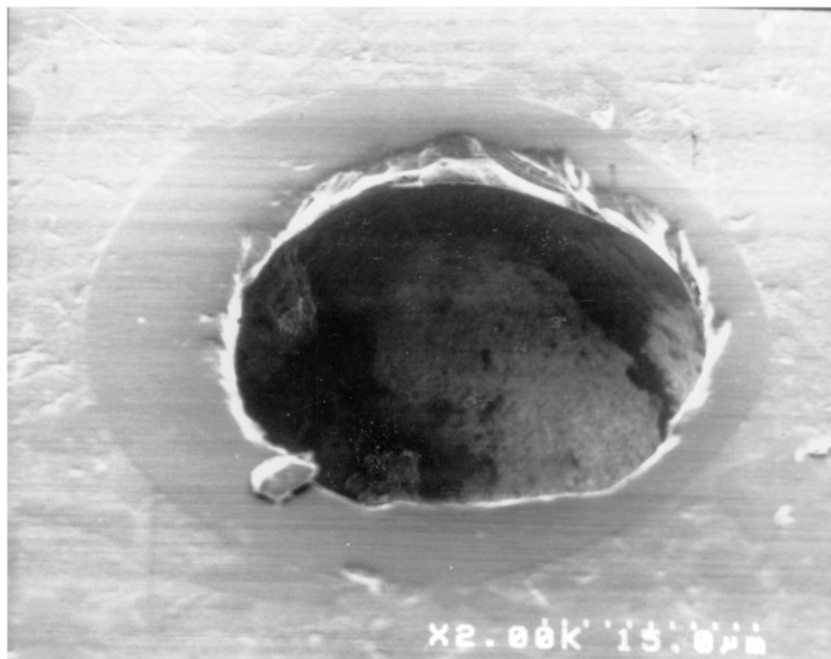
spheroidal and range in size up to  $\sim 100 \mu\text{m}$ , i.e., much larger than the fiber diameter of  $\sim 5 \mu\text{m}$ . In general, the thick walled particles are usually hollow (Figs 2a and 3a), while about 99.5 percent of the thin walled particles are filled with the matrix alloy (Fig. 1). These filled thin wall particles are of course harmless from the fatigue viewpoint; only the empty ones act as crack initiators.

The two types of composite contained particles with a similar range of particle diameter but a substantially different range of wall thicknesses. From a stiffness or strength viewpoint, it is appropriate to classify the particles in terms of the ratio of the wall thickness ( $t$ ) to

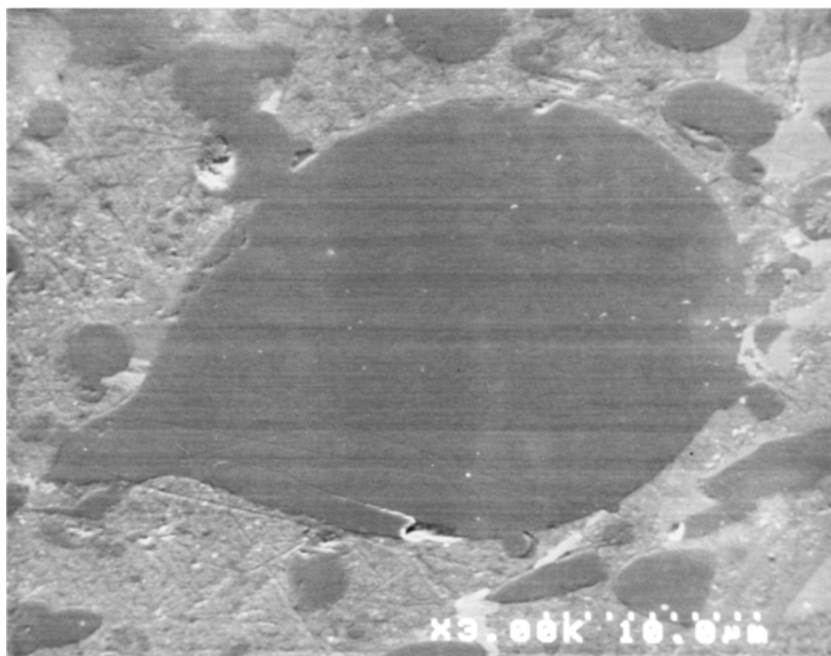
the particle radius ( $a$ ). The Type I composites contained particles with  $t/a$  as small as 0.02, whereas in the Type II composites, the smallest value of  $t/a$  was 0.2. So it is convenient to divide the particles into two categories on this basis i.e.,

- Thin walled particles with  $t/a \leq 0.2$  (e.g., Fig. 1)
- Thick walled or solid particles with  $t/a \geq 0.2$  (e.g., Figs 2 and 3)

The surface concentrations of these two categories of shot particle are summarized in Table I. Type II composites contained a smaller concentration of both



(a)



(b)

Figure 3 Scanning electron micrographs of a Type II composite showing: (a) a hollow thick-walled shot particle and (b) a solid shot particle.

types of particle than the Type I composites. Particularly noteworthy is that Type II did not contain any of the thin walled particles, which are so abundant in Type I.

TABLE I Surface concentrations ( $\text{mm}^{-2}$ ) of shot particles observed on polished sections of Kaowool/339 aluminum composites

Composite	Thick walled <sup>a</sup> or solid shot particles	Thin walled <sup>b</sup> shot particles
Type I	1.0	1.0
Type II	0.65	0

<sup>a</sup>Thick wall =  $ta > 0.2$ .

<sup>b</sup>Thin wall =  $ta < 0.2$ .

#### 4. Fatigue performance

The fatigue life at 300°C is shown as a function of cyclic stress (i.e., S-N curve) in Fig. 4. The Type I composites exhibit a large scatter in fatigue life, whereas the Type II fatigue lives are clustered very closely and coincide with the best (i.e., longest lived) of Type I. The Type I composites are the same as those described previously [3], in that many failures originated at a hollow thin walled shot particle located close to the surface. Since this behavior was well documented previously [3], it suffices here to illustrate with a typical example such as that shown in the scanning electron micrograph on Fig. 5. The fatigue life is reduced substantially by these surface particles. If the particle is substantially

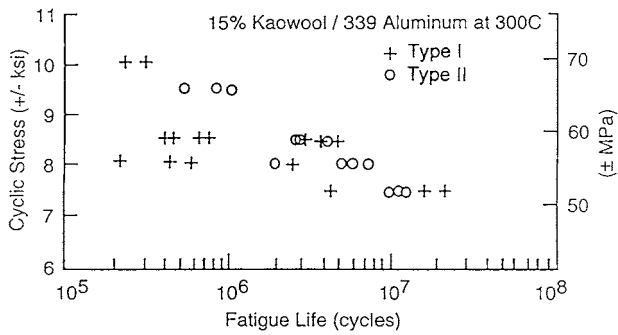


Figure 4 Relationship between the applied cyclic stress and the number of cycles to failure for 15% Kaowool/339 aluminum composites at 300°C.

subsurface or filled with the matrix alloy, the fatigue life is much longer and similar to that for the Type II composites. Thus, the wide scatter in fatigue lives originated primarily from variations in the proximity of hollow thin walled shot particles to the free surface and this dominating factor again obscured any effect of particle size. In the case of the Type II composites, the location of crack initiation was clearly defined on the fracture surface, but no shot particle or other defect could be identified. This is consistent with the very small scatter in fatigue life.

Again, note that both types of composite contain shot particles. The important difference between them is that Type I contain shot particles with  $t/a$  as small as 0.02, whereas in the Type II  $t/a \geq 0.2$ . An analysis of this important effect of wall thickness is presented in the next section.

## 5. Model

A 3D model of a hollow shot particle was developed following the same format as our 2D model described previously [3]. A cross sectional view of a spherical particle at a distance  $d$  from the surface is shown schematically in Fig. 6a. The particle has an outside radius  $a$  and a wall thickness  $t$ . Fig. 6b depicts the case of a particle,

which has been partially removed during machining so that the hollow cavity is exposed at the surface. The location of such a particle is described by negative values of  $d$ , e.g.,  $d = -a$  corresponds to a hemispherical particle at the surface. As indicated in Fig. 6, the uniaxial applied stress  $P$  is parallel to the surface. The value of  $P = 60$  MPa was chosen to simulate the condition existing during a typical uniaxial fatigue test at 300°C (Fig. 4). At this temperature the residual stresses are only  $\sim 10$  MPa [5] so are not included in the model.

The analysis of both the 2D and 3D models was performed by the finite element method using commercially available software Ansys 5.1 [6]. The portions of the finite element mesh occupied by the Kaowool and the aluminum matrix were assigned the values of modulus and Poisson's ratio listed in Table II. Note that the modulus chosen for aluminum is the value at 300°C [7, 8]. The plasticity of the aluminum matrix was incorporated by assuming that it obeyed the stress-strain relationship measured for the unreinforced 339 aluminum at 300°C (Fig. 7).

While a 3D finite element model is a more accurate representation than a 2D model, it is also more complex, so only three geometries were investigated; namely, those considered to be the most significant on the basis of the earlier 2D-study [3]. These are:

- A particle remote from the surface ( $d = 2a$ ), which provides a baseline for comparison with the other geometries
- A particle at the surface, i.e.,  $d = 0$
- A fractional particle at the surface, i.e., one which retains 95% of the diameter of the internal cavity of the particle after machining

Our earlier 2D model showed that the important locations of stress concentration are at A and C in the Kaowool and at D in the aluminum matrix (see Fig. 6). Since this is also true for the 3D model, the results are again restricted to these three locations.

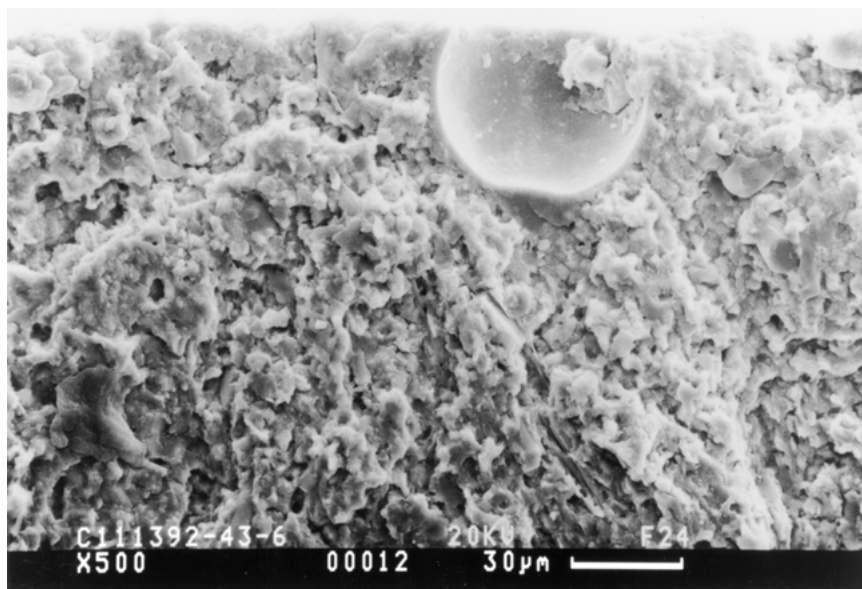
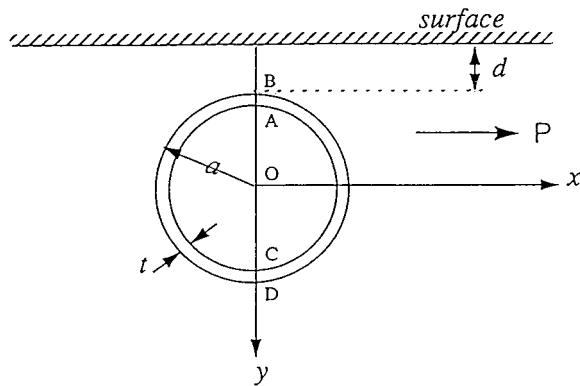


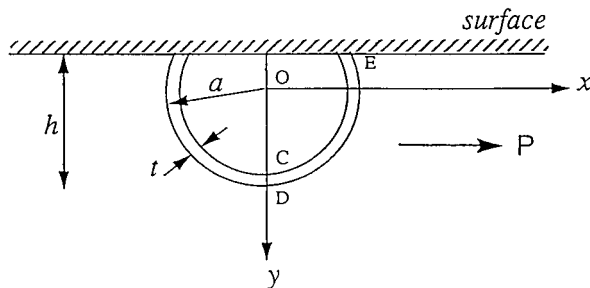
Figure 5 Scanning electron micrograph of a typical hollow shot particle responsible for crack initiation in the Type I composites.

TABLE II Elastic properties of Kaowool and aluminum

	Kaowool	Aluminum
Young's modulus (GPa)	120	50
Poisson's ratio	0.2	0.347



(a) Spherical particle beneath the surface



(b) Partial particle left at the surface after machining

Figure 6 Schematic cross section of spherical hollow shot particles: (a) particle beneath the surface and (b) fractional shot particle left at surface after machining.

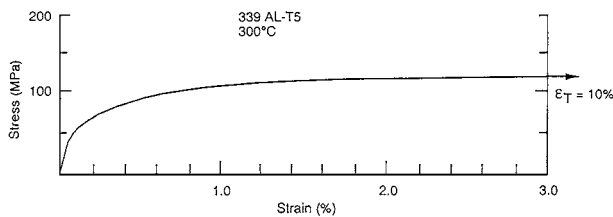


Figure 7 Engineering stress vs. engineering strain during tensile deformation of unreinforced 339 Al at 300°C.

In the more complete 3D model incorporating matrix plasticity, a plastic zone develops in the matrix adjacent to the particle and encompasses a wide range of stresses and plastic strains. From the viewpoint of fatigue of the matrix alloy, the localized plastic strain is considered to be a fundamental parameter, but for our present purposes, it is more straightforward to follow our previous description in terms of localized stresses. In the 3D model these stresses are hydrostatic, but the dominant component at the three stress maxima A, C, and D is parallel to the applied stress. So we again simplify our analysis by representing the results in terms

of the stress component  $\sigma_{xx}$ . This approach provides a direct comparison of the 2D and 3D models and more importantly enables the role of a particle under fatigue loading to be defined simply by comparing the value of  $\sigma_{xx}$  in the matrix with the applied uniaxial stress  $P = 60$  MPa, viz.

- If  $\sigma_{xx} < 60$  MPa, the particle acts as a reinforcement
- If  $\sigma_{xx} > 60$  MPa, the particle acts as a defect

## 6. Effect of distance from surface

A preliminary verification of the predictions of our 3D model is provided by a comparison with those of the 2D model, for the case of a particle with a wall thickness  $t = 0.1a$ , which is typical of those which act as crack initiators. As the particle approaches the surface, the stresses in the Kaowool and in the adjacent aluminum matrix increase substantially. This is illustrated in Fig. 8, which also shows the effect of including the plasticity of the matrix. The predictions of the 2D and 3D models have the following common qualitative features:

- The stress in the Kaowool at A increases to a large value when  $d = 0$  (Fig. 8a)
- The stresses in the Kaowool at C (Fig. 8b) and the matrix at D (Fig. 8c) attain a maximum value for a fractional particle ( $d < 0$ )
- The incorporation of matrix plasticity into either model increases the stresses in the Kaowool and decreases the stresses in the matrix
- When such a thin walled particle is close to the surface, all four conditions of the model predict that the stress in the matrix will exceed the applied stress (Fig. 8c), i.e., the particle acts as a defect.

However, in comparison to the 2D model, the 3D model predicts larger stresses in the Kaowool (Figs 8a and b) and smaller stresses in the aluminum matrix (Fig. 8c).

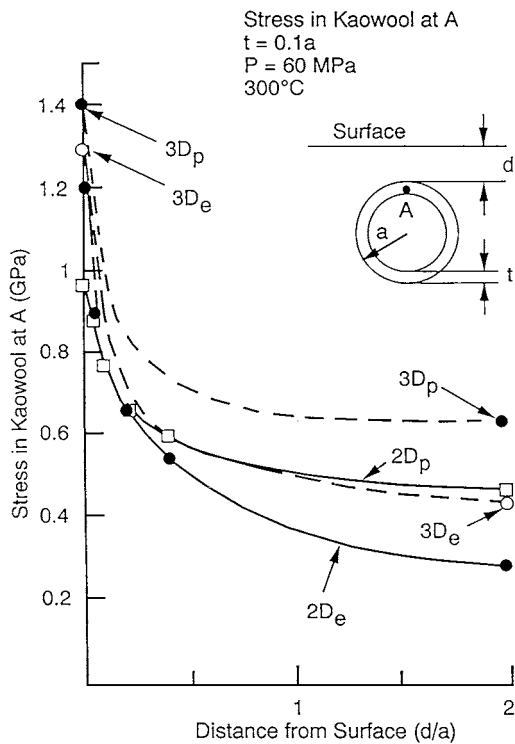
In fact, for the 3D elastic plastic model, the calculated stress in the Kaowool at A and C exceeds the ultimate tensile strength of Kaowool (1.4 GPa [9]).

## 7. Effect of wall thickness

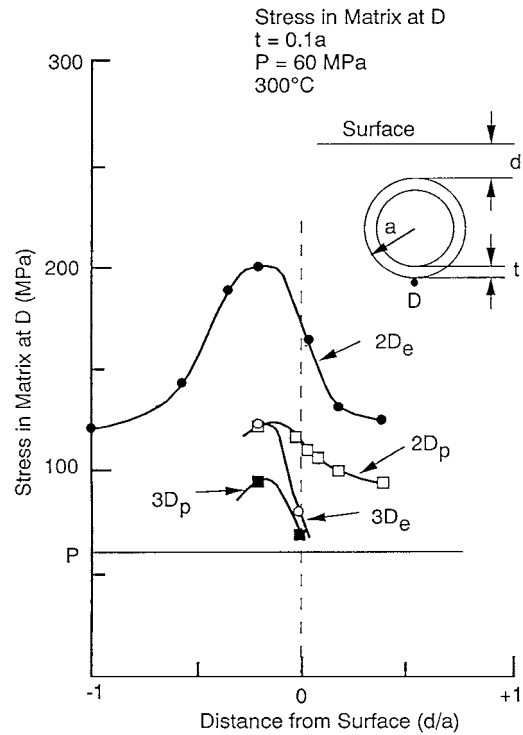
It is important to consider the effect of wall thickness on the stresses in both the aluminum matrix and the Kaowool.

### 7.1. Stress in matrix

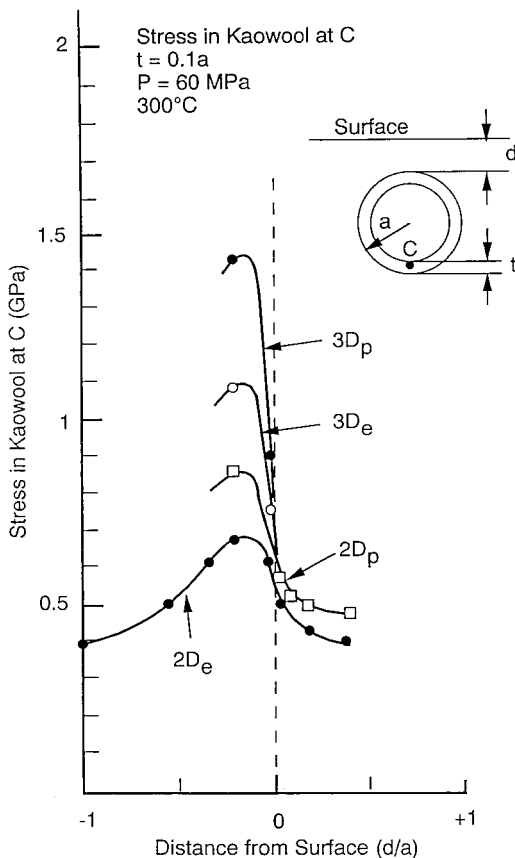
The stress in the aluminum matrix at D decreases with increasing particle wall thickness. This important effect is illustrated for a subsurface particle at  $d = 2a$  in Fig. 9a, for a particle at the surface ( $d = 0$ ) in Fig. 9b, and for a fractional particle in Fig. 9c. Each of these figures again shows that the calculated stresses for the 3D model are substantially smaller than those for the 2D model, and that the stresses are decreased by the incorporation of matrix plasticity. However, the most



(a)



(c)



(b)

Figure 8 Effect of the proximity of a shot particle to the free surface on the stress  $\sigma_{xx}$ : (a) in the Kaowool at location A, (b) in the Kaowool at location C, and (c) in the aluminum matrix at location D. The four curves in each case show the values calculated from the 2D and 3D models, both with (e.g., 3D<sub>p</sub>) and without (e.g., 3D<sub>e</sub>) matrix plasticity.  $t = 0.1a$ ,  $P = 60$  MPa. (Continued)

Figure 8 (Continued)

important feature of these figures is the intersection of each curve with the horizontal line corresponding to the applied stress of 60 MPa. This intersection defines a critical value of wall thickness corresponding to the transition in the role of the particle from defect to reinforcement. The calculated values of critical wall thickness ( $t_c$ ) are summarized in Table III. It is clear that the 3D model predicts substantially smaller values of  $t_c$  than does the 2D model and that the inclusion of matrix plasticity also decreases the value of  $t_c$ . For each of the four modeling conditions considered, the dependence on particle location is very similar with the largest value of  $t_c$  corresponding to the fractional particle. The 3D model with plasticity provides the most accurate values of  $t_c$ ; of these the most critical is  $t_c = 0.18a$  for the fractional particle.

## 7.2. Stress in Kaowool

The stress in the Kaowool at A attains a maximum value when  $d = 0$  (Fig. 8a). The effect of wall thickness on this maximum stress is shown in Fig. 10a. Similarly, the stress in the Kaowool at C attains a maximum value

TABLE III Calculated values of critical wall thickness ( $t/a$ ) (from Fig. 9)

Model	Embedded ( $d = 2a$ )	at Surface ( $d = 0$ )	Fractional ( $d = -0.95$ )
2D elastic	0.28	0.4	0.65
2D elastic/plastic	0.18	0.26	0.32
3D elastic	0.17	0.21	0.32
3D elastic/plastic	0.07	0.12	0.18

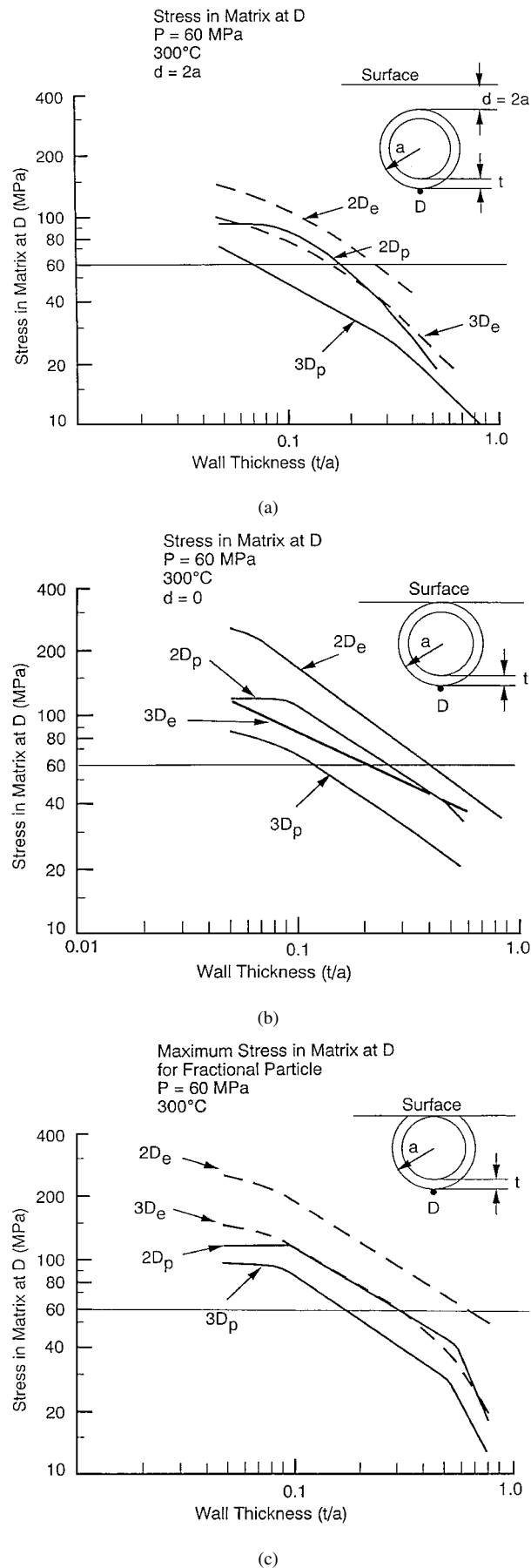


Figure 9 Effect of particle wall thickness on the stress  $\sigma_{xx}$  in the aluminum matrix at D: (a) when the particle is subsurface ( $d = 2a$ ), (b) when the particle touches the surface ( $d = 0$ ), and (c) for a fractional particle ( $d = -0.95a$ ). The four curves in each case show the stresses calculated from the 2D and 3D models both with and without matrix plasticity,  $P = 60 \text{ MPa}$ .

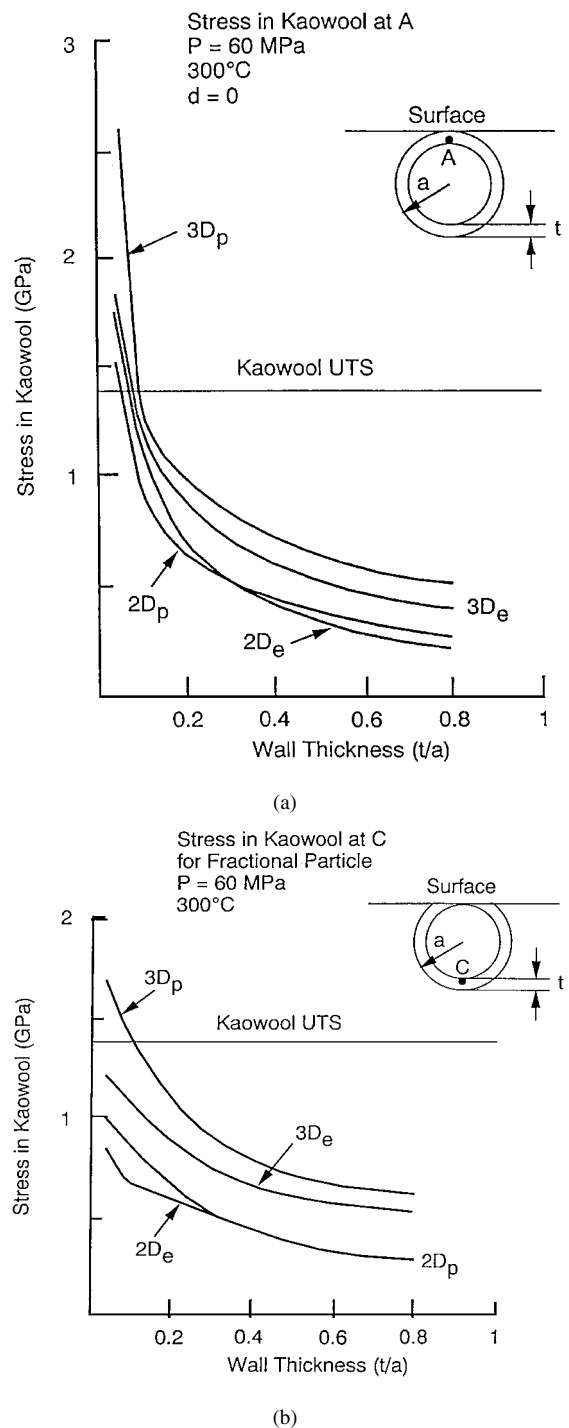


Figure 10 Effect of particle wall thickness on the stress  $\sigma_{xx}$  in the Kaowool: (a) at location A for a particle at the surface ( $d = 0$ ) and (b) at location C for a fractional particle at the surface ( $d = -0.95a$ ). The four curves in each case show the stresses calculated from the 2D and 3D models, both with and without matrix plasticity.  $P = 60 \text{ MPa}$ .

for the fractional particle geometry (Fig. 8b). The effect of wall thickness on this maximum value is shown in Fig. 10b. In both cases in Fig. 10, the 3D model predicts the higher stresses, which are increased further by the addition of matrix plasticity, attaining values exceeding the ultimate tensile strength of Kaowool (1.4 GPa).

## 8. Discussion

The important result of this study is that the Type II composites provide elevated temperature fatigue

properties superior to those of Type I. The latter exhibit considerable scatter in fatigue life due to crack initiation at hollow Kaowool shot particles, whereas the fatigue life of the Type II composites is quite well defined and no shot particles are found at the fracture origin. Although both types of composites contain shot particles, the important difference between them is the range of the ratio of the wall thickness ( $t$ ) to particle radius ( $a$ ). The Type I composites contain shot particles with  $t/a$  as small as 0.02, whereas in the case of the Type II  $t/a \leq 0.2$ .

The crucial role of particle wall thickness is clearly defined qualitatively by both the 2D and 3D finite element models, namely, that the stresses in both the Kaowool particle (Fig. 10) and the aluminum matrix (Fig. 9) increase as the wall thickness decreases. This effect of wall thickness is even more important when the stresses have already increased due to the proximity of the particle to the surface (Fig. 8), the largest stresses being associated with a particle, which had been partially removed during machining exposing an otherwise intact fractional particle at the surface.

Of particular significance are the stresses in the matrix because they demonstrate very clearly that thin walled particles act as defects, while thick walled particles act as reinforcements. Furthermore, this transition is defined by a critical value of wall thickness  $t_c$ , corresponding to the condition when the overall stiffness of the particle equals that of an equivalent volume of matrix aluminum. It is in this regard that the quantitative differences between the predictions of the 2D and 3D models are very important. In comparison to the 2D model, the 3D model predicts smaller stresses in the aluminum matrix, but larger stresses in the Kaowool. (An effect which is accentuated further by the incorporation of matrix plasticity.) Consequently, the 3D-elastic/plastic model predicts critical wall thicknesses which are much smaller than those obtained from a 2D model. This applies to all particle locations (Table III). For the worst-case scenario, namely a fractional particle exposed at the surface during machining, the 2D elastic model predicts  $t_c = 0.65a$  whereas the 3D elastic/plastic model predicts  $t_c = 0.18a$ . Similarly for a particle at the surface the 3D model predicts  $t_c = 0.12a$ . These values of critical wall thickness are in good agreement with our experimental observation, namely, that for the Type II composites wherein  $t \geq 0.2a$ , the fatigue failures did not originate at shot particles.

The 3D elastic/plastic model also predicts that for  $t < 0.1a$  the stresses in the Kaowool can exceed the ultimate tensile strength (UTS) of 1.4 GPa (Fig. 10), so that the failure could initiate in the shot particle itself during the first fatigue stress cycle. However, this is rather a moot point because for  $t < 0.1a$ , the stress in the matrix can exceed 90 MPa (Fig. 9), which corresponds to a strain of 0.5% (Fig. 7), and is more than sufficient to initiate the fatigue process.

Finally, we recognize that our simple model of a hollow perfectly spherical shot particle with a uniform wall thickness is rather idealistic, in that many particles are somewhat oblate with non-uniform wall thick-

ness (Figs 1 and 2). So, it is appropriate to consider the underlying physical basis of its success in accounting for the experimental observations. The key is provided by the fact that 99.5% of the shot particles are fractured and filled with the molten aluminum matrix alloy during squeeze casting (as in Figs 1 and 2), rendering them ineffective as sites for fatigue initiation. We can estimate which particles will be made harmless in this way by considering again our idealized hollow spherical particle immersed in molten aluminum under an applied external hydrostatic pressure ( $H$ ). A maximum tangential stress ( $\sigma$ ) is produced on the inner surface and is given by [10]

$$\sigma = -\frac{3}{2}H[1 - (1 - t/a)^3]^{-1} \quad (1)$$

If we assume that the compressive strength of the Kaowool shell equals the tensile strength of the Kaowool fibers (i.e., 1.4 GPa), which represents the worst case scenario (compressive strength in reality is larger than tensile strength for Kaowool ceramic), then for the pressure of 70 MPa applied during squeeze casting, particles with  $t/a < 0.03$  will fracture and be filled with aluminum. However, this limiting value will increase substantially for oblate particles and for those with non-uniform wall thickness. Thus, for the critical range of wall thickness, i.e.,  $0.03 < t/a < 0.18$ , the remarkable sphericity and uniformity of the particles which survive squeeze casting and cause fatigue failures (Fig. 5) can be understood.

## 9. Conclusions

1. The fatigue life of Kaowool/aluminum composites at 300°C is reduced by hollow spherical particles (shot) of Kaowool, which act as crack initiation sites particularly when located at the surface.
2. The ratio of the wall thickness ( $t$ ) to the particle radius ( $a$ ) is a crucial parameter: thin walled particles act as defects whereas thick walled particles act as reinforcements, the transition occurring at a critical wall thickness.
3. Finite element modeling predicts that the critical wall thickness increases as the particle approaches the free surface.
4. The largest stress concentrations occur for a surface particle which has been partially removed during machining. In this condition  $t_c = 0.18a$ .
5. Experimental confirmation is provided by the fatigue performance of two types of composites. In composites containing particles with wall thicknesses as small as  $0.02a$ , fatigue failures initiate at surface particles. In composites containing only particles with  $t > 0.2a$ , no particles are present at the fracture origin.

## Acknowledgments

The authors are grateful to S. M. Willett for the fatigue testing, to R. C. Lints and C. Wong for the scanning electron micrographs, and to C. Jones for the castings.

## References

1. W. J. BAXTER and A. K. SACHDEV, *Metall. and Mater. Trans. A* **30A** (1999) 815.
2. *Idem.*, *ibid.* **30A** (1999) 1835.
3. W. J. BAXTER, A. AL-OSTAZ and I. JASIUK, *ibid.* **30A** (1999) 195.
4. A. AL-OSTAZ, W. J. BAXTER and I. JASIUK, *J. Mater. Sci.* **36** (2001) 1201.
5. A. P. CLARKE and S. SAIMOTO, in "Micromechanics of Advanced Materials: Micromechanics of Deformation," edited by S. N. Chu, P. K. Liaw, R. J. Arsenault, K. Sadananda, K. S. Chan, W. Gerberich, C. Chau and T. Kung (TMS-AIME, Warrendale, PA, 1996).
6. ANSYS 5.1, Swanson Analysis Systems, Inc., Houston, PA.
7. "ASM Metals Handbook," p. 899.
8. "Aerospace Structural Metals Handbook" (Purdue University, 1995) Vol. 13.
9. Thermal Ceramics, Inc., Augusta, Georgia.
10. S. TIMOSHENKO and J. N. GOODIER, "Theory of Elasticity" (McGraw-Hill, New York, 1951).

*Received 6 September 2002  
and accepted 22 April 2003*